Journal of Theoretical and Applied Information Technology
20th September 2015. Vol.79. No.2

ISSN: 1992-8645 www.jatit.org E-ISSN: 1817-3195

GRID-CONNECTED PHOTOVOLTAIC SYSTEM USING AN ADVANCED BACKSTEPPING APPROACH

[1]KHALDI NAOUFEL, [2] MALIKA ZAZI, [3] HASSAN MAHMOUDI
[1,3] Mohammedia School of Engineer, Department of Electrical Engineering, Rabat, Morocco
[2] Higher School of Technical, Department of Electrical Engineering, Rabat, Morocco
E-mail: [1] naoufelkhaldi@gmail.com, [2] m.zazi@um5s.net.ma, [3] mahmoudi@emi.ac.ma

ABSTRACT

The objective of this paper is to present a nonlinear approach to design a suitable controller system for the photovoltaic (PV) single-phase grid-connected system. The system structure includes a PV generator, Boost converter, and DC-AC inverter coupled to grid network. A backstepping controller is developed to extract maximum point power tracking (MPPT), to regulate the DC bus voltage, and to generate a sinusoidal current into the grid in phase with grid voltage in order to achieve unity power factor. The stability of the control algorithm is demonstrated by tools of Lyapunov analysis. Simulations show that the proposed controller system completely accomplishes listed aims even under atmospheric conditions variation. The performance of the proposed controller has been validated by numerical simulation in MATLAB SIMULINK.

Keywords: *PV grid-connected system, backstepping technique, MPPT, power factor, Lyapunov stability*

1. INTRODUCTION

Demand for electrical energy has remarkably increased during the recent years with growing population and industrial progress. Since long time ago, fossil fuels have served as the major source of generating electrical energy. However the transfer of energy resulting from photovoltaic con-version remains relatively feeble. Therefore, many tracking control strategies have been proposed in existing literatures, such as perturb and observe[1], incremental conductance[2], neural net-work[3], and fuzzy logic methods[4]. Referring to [5][8], PV energy application can be divided into two modes, that is the stand-alone PV system and the PV grid-connected system. In detail, the stand-alone PV system requires battery banks to store the energy. On the other hand, the PV grid-connected system is used in distributed generation systems to deliver the power to the utility grid. In order to get a high-quality power and eliminate the harmonics distortion of current and voltage, various control strategy is proposed to solve this problems in a passivity-based control[9], and hysteresis current control [6], power controlled [7]. This paper results show that the proposed backstepping control can track maximum power point (MPP) in different temperature and irradiation, and to maintain the grid current with the grid voltage by ensuring the tight regulation of the DC-bus. The control inputs are the duty cycles of the boost converter and DC-AC inverter. The controller system in addition to achieve the mentioned objectives, it helps also to reduce the harmonic content of the network current and assure an excellent output characteristic of high accuracy and good robustness in front of system's perturbation.

The sequential work flow of this paper is as follows: the next section, mathematical modelling of a grid connected PV system has been described. Section 3 presents a controller design of the converters using a backstepping method. Simulation works in Matlab/Simulink, and results are discussed in Section 4. Lastly, in section 5, a precise conclusion has been added to finalize the work.

2. PV GRID-CONNECTED SYSTEM MODELLING

Figure 1 depicts the system configuration of the proposed single phase grid connected to the photo-voltaic array. It consists of PV connected to the DC bus via a boost converter, and then to the AC grid via a DC-AC inverter. The boost converter is used to increase the voltage level of PV array and to feed DC side of the inverter. The last one with filter inductor converts a DC input voltage into an AC sinusoidal, by changing the duty cycle of the switching inverter to inject the output current into the network with a power factor near unity.

Journal of Theoretical and Applied Information Technology
20th September 2015. Vol.79. No.2

ISSN: 1992-8645 www.jatit.org E-ISSN: 1817-3195

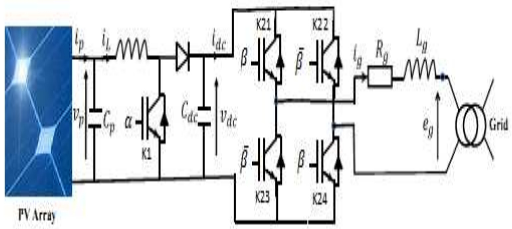

Figure 1: PV Single-Phase Grid-Connected System

2.1 PV Modelling

There are various methods to perform modeling work on the PV module, and the most of them is described by using mathematical modeling [2][3]. The equivalent circuit of a PV array can be depicted in Figure 2 where I_{ph} is current source of PV array, R_{sh} is an equivalent shunt resistance, R_s is an equivalent series resistance, i_p and v_p are the output current and output voltage of PV array, respectively. In general, for simplicity R_{sh} and R_s are assumed to be open circuit and short circuit, respectively. The simplified mathematical model of the output current is given as [2]:

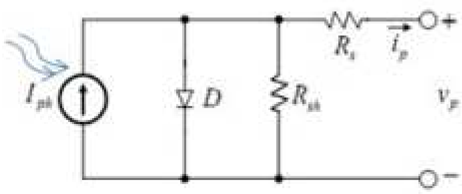

Figure 2: The Equivalent Circuit Of A PV Array

$$i_p = n_p I_{ph} - n_p I_{rs}\left[e^{\left(\frac{q}{pkn_s}\frac{v_p}{T}\right)} - 1\right] \quad (1)$$

Where q is the electron charge, k the Boltzmann's constant $(1.38 \times 10^{-23} J/K)$, p is the p–n junction ideality factor, T is the cell temperature, I_{rs} is the cell reverse saturation current, n_s is the number of solar cells connected in series, and n_p is the number of solar cells connected in parallel. In addition, the mathematical model of the reverse saturation current is given below:

$$I_{rs} = I_r\left(\frac{T}{T_{ref}}\right)^3 e^{\left[\left(\frac{qE_g}{pk}\right)\left(\frac{1}{T} - \frac{1}{T_{ref}}\right)\right]} \quad (2)$$

With

$$I_r = \frac{I_{SC}}{\left[e^{\left(\frac{v_{co}}{pn_s v_{tr}} \times \frac{v_p}{T}\right)} - 1\right]} \quad (3)$$

Where T_{ref} is the cell reference temperature, I_r is the reverse saturation current at T_{ref}, E_g is the band-gap energy of the semiconductor $(E_g \approx 1.1eV)$ and v_{tr} is a thermal potential at T_{ref}.

The current source of PV array I_{ph}, varied according to solar irradiation and cell temperature, is given below:

$$I_{ph} = [I_{sc} + K(T - T_{ref})] \times \left(\frac{E}{E_r}\right) \quad (4)$$

Where I_{sc} is short-circuit current at reference temperature and radiation, E is the solar irradiance and K, the temperature coefficient for short-circuit current. Using the equations 1 to 4 the PV panel can be modelled.

The table below represents the parameters of the PV module,is made by Shell solar company andproduct name is SP75.

TABLE 1: PARAMETERS OF SHELL SP75

Parameters	Values
Open Circuit Voltage(Voc)	21.7Volt
Short Circuit Current(Isc)	4.8Amp
Voltage at Pmax(Vmpp)	17Volt
Current at Pmax(Impp)	4.41Amp
Maximum Power (Pmpp)	75Watt
Number of Cell	36

The associated power-voltage and current-voltage characteristics curve under changing atmospheric conditions (irradiation and temperature) are shown in Figs. 3 and 4.

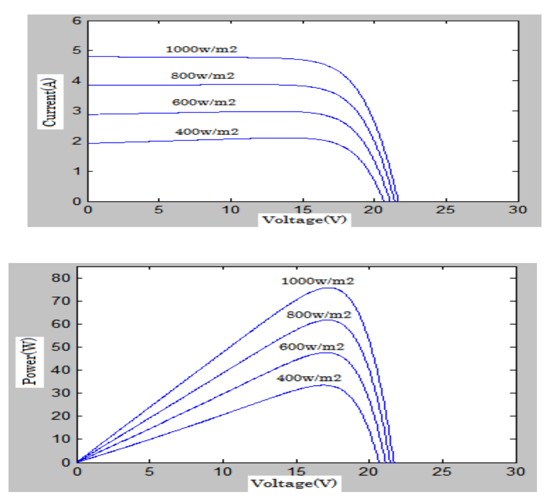

Fig. 3 I-V And P-V Characteristics Of Solar Module For Different Irradiance Level

ISSN: 1992-8645 www.jatit.org E-ISSN: 1817-3195

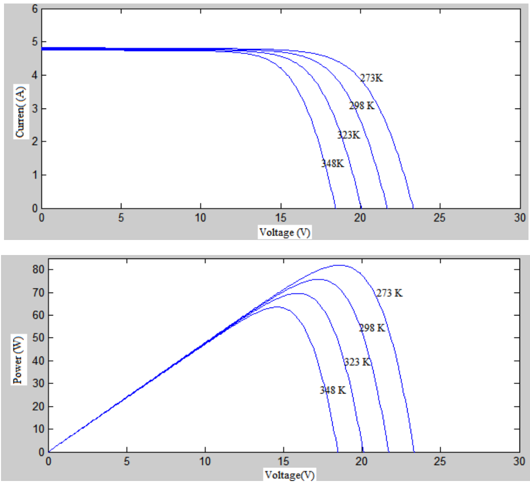

Fig. 4 I-V And P-V Characteristics Of Solar Module For Different Temperature

2.2 Single-phase Grid-connected PV System Modelling

As can be seen in Figure 1, the boost converter consists of the switch K1 controlled by a switching signal $\alpha_1 \in \{0,1\}$ (i.e., OFF or ON respectively) and the DC-AC inverter consists of four switches K21, K22, K23, K24 controlled by a switching signal $\beta_1 \in \{0,1\}$. The switching signal α_1 and β_1 can also be generated via a pulse-width modulation (PWM) scheme with an input signal α and $\beta \in [0,1]$ outputted by the controller. The development of the model switched system is based on the application of Kirchhoff's laws. Thus, we obtain:

$$\begin{cases} \frac{dv_p}{dt} = \frac{1}{C_p}\left(i_p - i_L\right) \\ \frac{di_L}{dt} = \frac{v_p}{L} - \frac{R}{L} i_L - \frac{v_{dc}}{L}(1-\alpha) \\ \frac{dv_{dc}}{dt} = \frac{i_L}{C_{dc}}(1-\alpha) - \frac{i_g}{C_{dc}}(2\beta-1) \\ \frac{di_g}{dt} = \frac{v_{dc}}{L_g}(2\beta-1) - \frac{R_g}{L_g} i_g - \frac{e_g}{L_g} \end{cases} \quad (5)$$

Where v_p, i_p, i_L, v_{dc}, e_g, and i_g are respectively, the average values over switching period of the PV voltage, PV current, boost inductor current, DC bus voltage, grid voltage, and grid current. C_p is the input capacitor, L is the inductor of the boost converter and R is the equivalent series resistance of the inductor. C_{dc} is the DC link capacitor, L_g is the filter inductor and R_g is the equivalent series resistance of the filter inductor. The control inputs α and β are duty cycles of the switching signals α_1 and β_1.The grid voltage $e_g = A\sin(\omega t)$ with a constant amplitude A and a constant frequency $\omega = 2\pi f$.

3. BACKSTEPPING CONTROLLER DESIGN

The aim of this section is developing a nonlinear controller that will be able to: (i) achieve the MPPT even with variations of irradiation and PV array temperature, (ii) ensure the regulation of the DC bus voltage, (iii) inject a sinusoidal current with a good quality in the network, which proves a power factor close to unity.

Figure 5 depict the structure of whole controlled system. The MPPT controller and power factor correction (PFC) controller will be synthesized using backstepping approach [10][11], and the DC voltage will be regulated by a simple proportional-integral corrector.

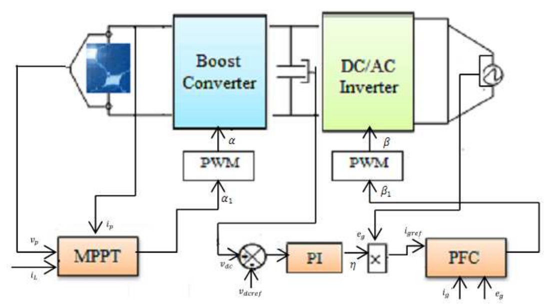

Figure 5: Control scheme of the whole system

3.1 MPPT Controller

The key goal of the MPPT Controller module is to extract maximum available power from PV array for any specific environmental variation. This is done with the help of an appropriate duty cycle signal α used to regulate the controlled output $z_1 = \frac{\partial P}{\partial v_p}$ of photovoltaic array to its reference $z_{1ref} = \frac{\partial P}{\partial v_p}|_{MPP} = 0$ in order to drive boost converter to achieve the MPP.

Design step 1

Let us introduce the following tracking error:

$e_1 = z_1 - z_{1ref}$

where

$$z_{1ref} = \frac{\partial P}{\partial v_p}|_{MPP} = \frac{\partial\left(v_p i_p\right)}{\partial v_p} = i_p + v_p\frac{\partial i_p}{\partial v_p} = 0 \quad (6)$$

Journal of Theoretical and Applied Information Technology
20th September 2015. Vol.79. No.2

ISSN: 1992-8645 www.jatit.org E-ISSN: 1817-3195

Using 5 and 6 , time derivation of e_1, we obtained the following error dynamics:

$$\dot{e}_1 = \left[i_p + \frac{\delta i_p}{\delta v_p} v_p\right] \ddot{v}_p \frac{\delta t}{\delta v_p} + \left[\frac{\delta i_p}{\delta v_p} + \frac{\partial^2 i_p}{\partial v_p^2} \times v_p + \frac{\delta i_p}{\delta v_p}\right]\left[\frac{1}{C_p}(i_p - i_L)\right] \tag{7}$$

Treating the boost inductor current i_L as a virtual control input, with respect to candidate Lyapunov function $V_1 = \frac{1}{2}e_1^2$ indeed, its time derivative is given by:

$$\dot{V}_1 = e_1\left(\left[i_p + \frac{\delta i_p}{\delta v_p} v_p\right] \ddot{v}_p \frac{\delta t}{\delta v_p} + \left[\frac{\delta i_p}{\delta v_p} + \frac{\partial^2 i_p}{\partial v_p^2} \times v_p + \frac{\delta i_p}{\delta v_p}\right]\left[\frac{1}{C_p}(i_p - i_L)\right]\right) \tag{8}$$

In the above equation, if we chose $X_1 = (I_L)_d$ as a virtual control variable, where $(I_L)_d$ is the desired value of the boost inductor current, we can find the following stabilizing function of e_1 :

$$-C_1 e_1 = \left(\left[i_p + \frac{\delta i_p}{\delta v_p} v_p\right] \ddot{v}_p \frac{\delta t}{\delta v_p} + \left[\frac{\delta i_p}{\delta v_p} + \frac{\partial^2 i_p}{\partial v_p^2} \times v_p + \frac{\delta i_p}{\delta v_p}\right]\left[\frac{1}{C_p}(i_p - X_1)\right]\right) \tag{9}$$

Where C_1 is a positive design parameter. The desired value X_1 called stabilization function, is given by :

$$X_1 = i_p + \left(C_p \frac{1}{\left[\frac{\delta i_p}{\delta v_p} + \frac{\partial^2 i_p}{\partial v_p^2} \times v_p + \frac{\delta i_p}{\delta v_p}\right]}\right)\left(C_1 e_1 + \left(\left[i_p + \frac{\delta i_p}{\delta v_p} v_p\right] \ddot{v}_p \frac{\delta t}{\delta v_p}\right)\right) \tag{10}$$

Design step 2

As i_L is not the actual control input, a new error variable $e_2 = i_L - X_1$, between the virtual control and its desired value X_1 should be vanish, then according to 5 and 7, we obtain :

$$\dot{e}_2 = \frac{v_p}{L} - \frac{R}{L} - \frac{v_{dc}}{L}(1-\alpha) - \dot{X}_1 \tag{11}$$

$$\dot{e}_1 = \left[i_p + \frac{\delta i_p}{\delta v_p} v_p\right] \ddot{v}_p \frac{\delta t}{\delta v_p} + \left[\frac{\delta i_p}{\delta v_p} + \frac{\partial^2 i_p}{\partial v_p^2} \times v_p + \frac{\delta i_p}{\delta v_p}\right]\left[\frac{1}{C_p}(i_p - (e_2 + X_1))\right] \tag{12}$$

and adding 10, we defind $\dot{e}_1$ and $\dot{V}_1$:

$$\dot{e}_1 = -\frac{1}{C_p}\left[\frac{\delta i_p}{\delta v_p} + \frac{\partial^2 i_p}{\partial v_p^2} \times v_p + \frac{\delta i_p}{\delta v_p}\right] - C_1 e_1 \tag{13}$$

$$\dot{V}_1 = -\frac{1}{C_p}\left[\frac{\delta i_p}{\delta v_p} + \frac{\partial^2 i_p}{\partial v_p^2} \times v_p + \frac{\delta i_p}{\delta v_p}\right] e_1 - C_1 e_1^2 \tag{14}$$

Time derivative of the stabilising function X_1 is the following:

$$\dot{X}_1 = \left[\frac{\partial i_p}{\partial t} + C_p\left(\frac{(C_1 \dot{e}_1 + e_1)}{\left(\frac{\delta i_p}{\delta v_p} + \frac{\partial^2 i_p}{\partial v_p^2} \times v_p + \frac{\delta i_p}{\delta v_p}\right)} - \frac{C_1 e_1}{\left(\frac{\delta i_p}{\delta v_p} + \frac{\partial^2 i_p}{\partial v_p^2} \times v_p + \frac{\delta i_p}{\delta v_p}\right)^2}\left(2\frac{\delta^2 i_p}{\delta v_p^2} + \frac{\partial^3 i_p}{\partial v_p^3} \times v_p + \frac{\delta^2 i_p}{\delta v_p^2}\right)\frac{\partial v_p}{\partial t}\right)\right] \tag{15}$$

Consider the augmented candidate Lyapunov function:

$$V_2 = V_1 + \frac{1}{2}e_2^2 \tag{16}$$

Time derivative of V_2 is given as follows:

$$\dot{V}_2 = e_2\left[-\frac{1}{C_p}\left(\frac{\delta i_p}{\delta v_p} + \frac{\partial^2 i_p}{\partial v_p^2} \times v_p + \frac{\delta i_p}{\delta v_p}\right)e_1 + \frac{1}{L}(R - v_p - v_{dc}) + \frac{v_{dc}}{L}\alpha - \dot{X}_1\right] - C_1 e_1^2 \tag{17}$$

The control law α which guarantees the global stability with respect to candidate Lyapunov function as follows :

$$\alpha = \frac{L}{v_{dc}}\left[\frac{1}{C_p}\left(\frac{\delta i_p}{\delta v_p} + \frac{\partial^2 i_p}{\partial v_p^2} \times v_p + \frac{\delta i_p}{\delta v_p}\right)e_1 - \frac{1}{L}(R - v_p - v_{dc}) + \dot{X}_1 - C_2 e_2\right] \tag{18}$$

Where $C_2 > 0$ being a design parameterthe dynamics of Lyapunov function is reduced to:

$$\dot{V}_2 = -C_1 e_1^2 - C_2 e_2^2 < 0 \tag{19}$$

this vector error (e_1, e_2) ensures that the $e_1 = z_1 - z_{1ref}$ converges asymptotically to the origin. Therefore, the MPPT is achieved.

3.2 PFC Controller

As can be seen in Figure 3, to attain the unity power factor, it is necessary to regulate the DC link voltage v_{dc} to its desired value v_{dcref} via an outer voltage control loop. Moreover, there is an inner control loop in cascade which generates an output current in phase with the grid voltage and ensures a low current harmonics. The grid current i_g should reach a reference signal i_{gref} through the inner control loop:

$$i_{gref} = \eta e_g = \eta A \sin(\omega t) \tag{20}$$

η is a tuning parameter adjusted by the following PI control law:

$$\eta(t) = C_3\left(v_{dc}(t) - v_{dcref}(t)\right) + C_4\int_0^t \left(v_{dc}(\tau) - v_{dcref}(\tau)\right)d\tau \tag{21}$$

Where C_3 and C_4 are respectively the proportional and integral gain.

Let us introduce the following current error $e_3 = z_2 - z_{2ref}$, its dynamics becomes:

ISSN: 1992-8645 www.jatit.org E-ISSN: 1817-3195

$$\dot{e}_3 = \frac{v_{dc}}{L_g}(2\beta - 1) - \frac{R_g}{L_g}i_g - \frac{e_g}{L_g} - \frac{di_{gref}}{dt} \quad (22)$$

Consider the candidate Lyapunov function $V_3 = \frac{1}{2}e_3^2$, and its derivative with respect to time is given by :

$$\dot{V}_3 = e_3\left[\frac{v_{dc}}{L_g}(2\beta - 1) - \frac{R_g}{L_g}i_g - \frac{e_g}{L_g} - \frac{di_{gref}}{dt}\right] \quad (23)$$

We deduce then the following stabilizing control law:

$$\beta = \left[-C_5e_3 + \frac{R_g}{L_g}i_g + \frac{e_g}{L_g} + \frac{di_{gref}}{dt} + \frac{v_{dc}}{L_g}\right]\frac{L_g}{2v_{dc}} \quad (24)$$

4. SIMULATON RESULTS

In order to investigate the performance of the proposed backstepping control algorithm, a numerical simulation was made in the environment Matlab/Simulink. The system characteristics and controller parameters are summarized in table 2. Two cases were selected to demonstrate the design results. In the first one, the solar radiation changes its value as follows: 500W/m^2 to 1000W/m^2 at t = 1.5s while the temperature is kept constant at 298K. In the second case, the temperature has variable values as follows: 273K to 298K at t = 1.5s while the solar radiation is kept constant at 1000W/m^2.Figures 6 to 13 gives the simulation results when the reference of the DC bus voltage v_{dc} is v_{dcref} = 24v .

Figures 6 and 10, show that the backstepping method deliver the suitable duty cycle signal used to drive boost converter to reach the MPP very quickly and with an excellent performances and high accuracy even with variations of atmospheric conditions.

Figures 7 and 11 illustrate respectively, the PV array voltage, the PV array current, the boost inductor current and the DC bus voltage, we note that a good concordance between theoretical values and thus output signal obtained by Matlab. It is noted also that the Dc link voltage v_{dc} is regulated to the set value v_{dcref} with a good efficiency.

Figures 8 and 12, show that the current and the grid voltage are in phase, and sinusoidal. As a result, the designed PV grid-connected system reaches unity power factor. They indicate also that the injected current to grid i_g tracks the reference value i_{gref}.

Finally in Figures 9 and 13, are presented the control signals α and β, it is clear that they are bounded.

Unfortunately, this method presents a limitation in terms of overall cost, as comparing with other techniques. Analog implementation is generally cheaper and less complex than its digital counterpart, which normally requires hardware like a number of sensors, software and programming.

Table 2: Parameters Of The Whole System

System characteristics	Controller parameters
$C_P = 47mF$	$C_1 = 50$
$C_{dc} = 4.7mF$	$C_2 = 1000$
$V_{dcref} = 24V$	$C_3 = 0.025$
$L = 3.5mH$	$C_4 = 1$
$L_g = 2.6mH$	$C_5 = 300$
$R_g = 0.47\Omega$	

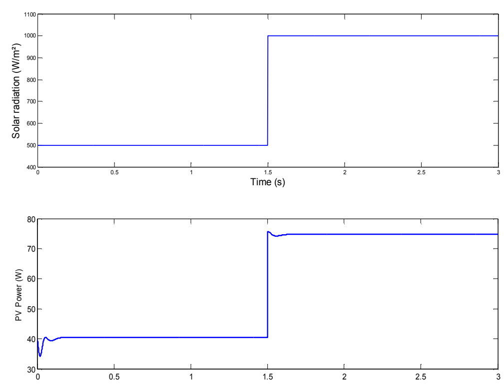

Figure 6: PV power with irradiation variation

ISSN: 1992-8645 www.jatit.org E-ISSN: 1817-3195

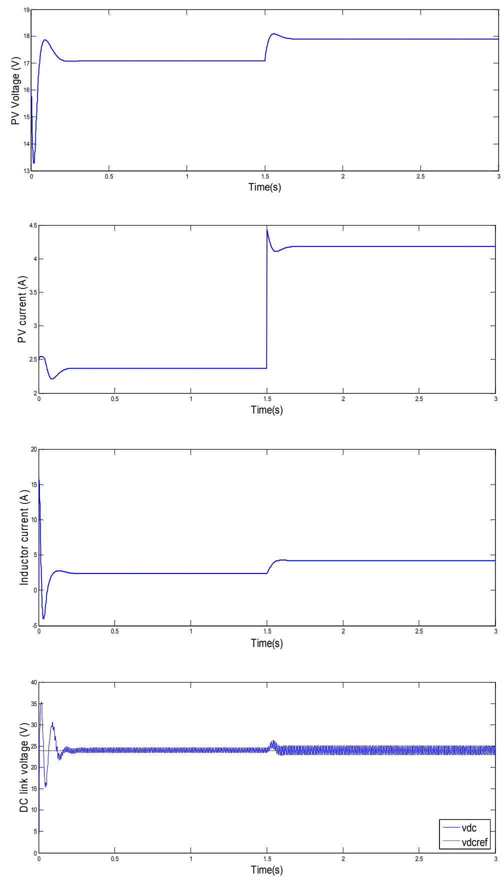

Figure 7: PV voltage, PV current, inductor current, DC link voltage

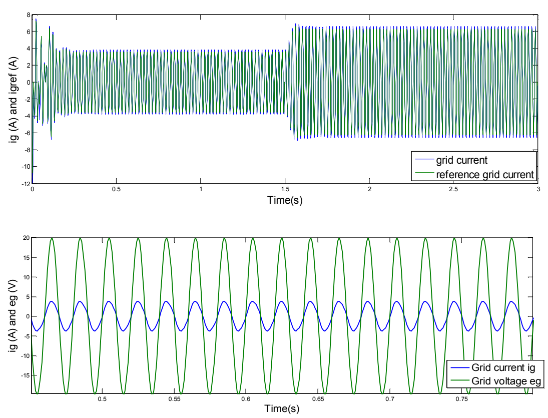

Figure 8: PFC cheeking and grid current with its reference

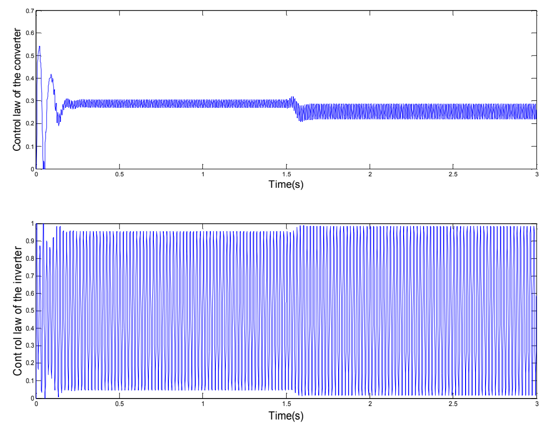

Figure 9: Control signals of the converter and inverter

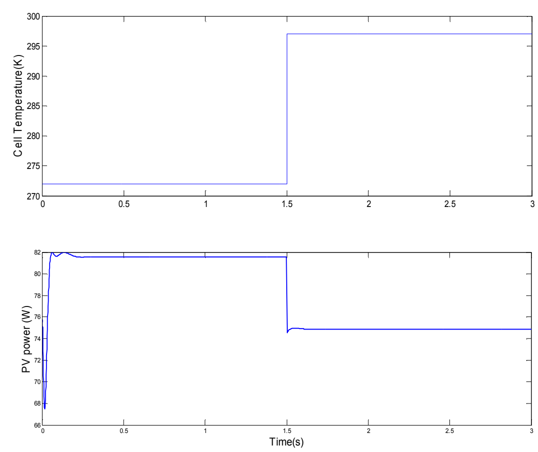

Figure 10: PV power with Temperature variation

ISSN: 1992-8645 www.jatit.org E-ISSN: 1817-3195

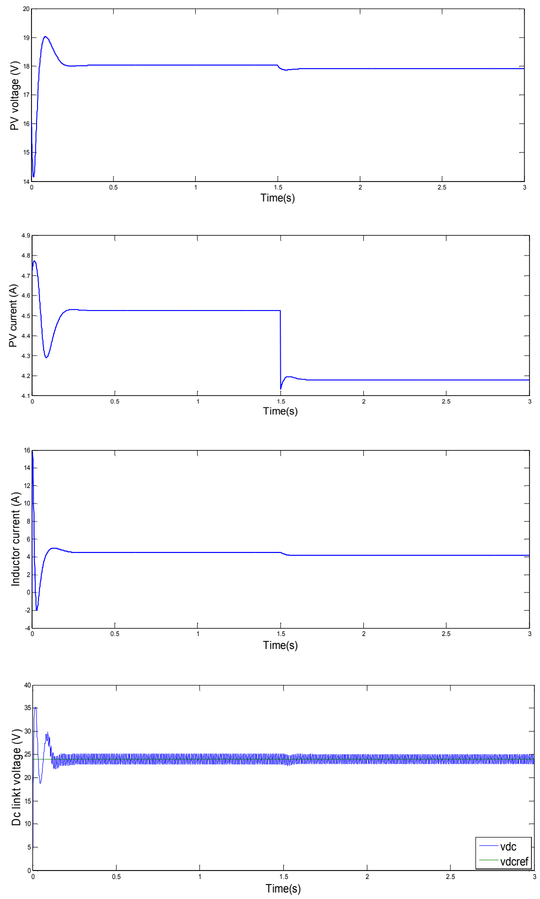

Figure 11: PV voltage, PV current, inductor current, DC link voltage

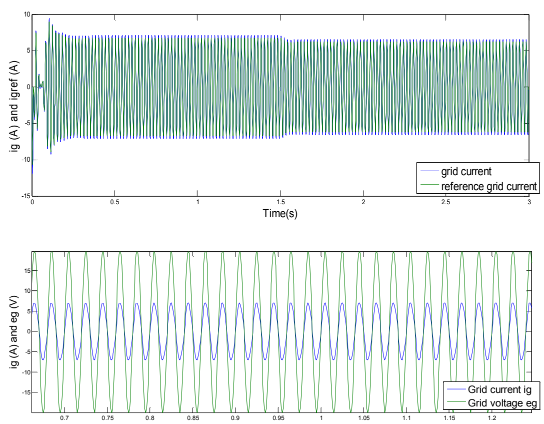

Figure 12: PFC cheeking and grid cur-rent with its reference

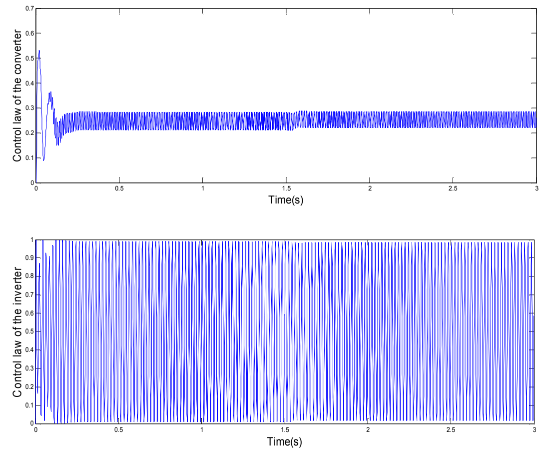

Figure 13: Control signals of the converter and inverter

5. CONCLUSION

In this paper, we presented an advanced nonlinear controller using backstepping strategy for PV system connected to grid. The proposed controller is developed to track the maximum power point from the PV array, to regulate the DC link voltage and to inject a suitable sinusoidal current in the grid with a unity power factor. The synthesis of the regulator was achieved by ensuring an asymptotic stability in the sense of Lyapunov. Simulation results under Matlab/Simulink prove that the controller guarantees a satisfactory performance and high efficiency even with a variation of irradiation and temperature.

REFRENCES:

[1] M.A.A. Mohd Zainuri, M.A. Mohd Radzi, Azura Che Soh and N. Abdul Rahim, "Comparative Analysis of the Perturb-and-Observe and Incremental Conductance MPPT Methods", *The 8th International Symposium On Advanced Topics In Elec-trical Engineering*, 2013.

[2] Tekeshwar Prasad Sahu, T. v. Dixit, "Modelling and Analysis of Perturb and Observe and Incremental Conductance MPPT Algorithm for PV Array Using Cuk Converter", *IEEE Student's Conference on Electrical, Electronics and Computer Science*, 2014, pp. 1–6.

[3] Naoufel Khaldi, Hassan Mahmoudi, Malika Zazi, Youssef Barradi, "Implementation of a MPPT Neural Controller for Photovoltaic Systems on FPGA Circuit", *WSEAS Transactions on power systems*. Vol. 9, 2014, pp. 471–478.

[4] M. Dilip Kumar, I. Deepa, "Implementation of

ISSN: 1992-8645 www.jatit.org E-ISSN: 1817-3195

fuzzy logic MPPT control and modified H-bridge inverter in photovoltaic system", *International Conference on Electronics and Communication Systems (ICECS),* 2014, pp. 1–6.

[5] H. Radwan, M. Orabi, "The non-ideality effect of optimizing the PO MPPT algorithm for PV Stand-alone applications", *IEEE the 34th International Conference on Telecommunications Energy (INTELEC)*, 2012, pp. 1–7.

[6] F. Zare, G.Ledwich, "A hysteresis current control for single-phase multilevel voltage source inverters: PLD implementation", *IEEE Transactions on Power Electronics*.Vol.17, 2002, pp. 731–738.

[7] Huijuan Li, Yan Xu, S.Adhikari, D.T. Rizy,Fangxing Li, P. Irminger, "Real and Reactive Power Control of a Three-Phase Single stage PV System and PV Voltage Stability", *IEEE Power and Energy Society General Meeting*. 2012, pp. 1–8.

[8] Jui-Liang Yang, Ding-Tsair Su, Ying-Shing Shiao, "Research on MPPT and Single stage Grid-Connected for Photovoltaic System", *WSEAS Trasactions On Systems.*Vol.7, 2008, pp. 1117–1131.

[9] G. Perez-Ladron, V. Cardenas, N. Visairo, F. Pazos, "Passivity-based control technique for UPS inverters" *European Control Conference (ECC)*, 2007, pp. 5734–5739.

[10] M.L. McIntyre, M. Schoen, ; J. Latham, "Back-stepping control of a capacitance-less photo-voltaic power converter with maximum power point tracking" *, IEEE 39th Photovoltaic Special-ists Conference (PVSC),* 2013, pp. 2908–2913.

[11] M. Honsberg, T. Radke, "3-level IGBT modules with trench gate IGBT and their thermal anal-ysis in UPS, PFC and PV operation modes" , *13th European Conference on Electronics Power and Applications, (EPE)*, 2009, pp. 1–7.